Journal of Visualization, Vol. 11, No. 1 (2008)45-54

Regular Paper

PIV Measurements on the Change of the Three-Dimensional Wake Structures by an Air Spoiler of a Road Vehicle

Kim, J. S.*[1], Sung, J.*[2], Kim, S.*[3] and Kim, J. S.*[3]

*1 Mechanical Engineering, Graduate School, Sunchon National University, 315 Maegok-dong, Suncheon, Jeonnam 540-742, Korea.
*2 Department of Mechanical Engineering, College of Engineering, Seoul National University of Technology, Gongreung 2-dong, Nowon-gu, Seoul 139-743, Korea. E-mail: jysung@snut.ac.kr
*3 School of Mechanical and Aerospace Engineering, College of Engineering, Sunchon National University, 315 Maegok-dong, Suncheon, Jeonnam 540-742, Korea.

Received 26 April 2007
Revised 15 September 2007

Abstract : The three-dimensional vortical structures formed in the wake behind a road vehicle were measured using a particle image velocimetry (PIV) technique and the change of the structures by the existence of an air spoiler was investigated. The measurements were carried out in several *x-y*, *y-z* and *z-x* planes to obtain full three-dimensional flow fields, including an out-of-plane velocity component, obtained by interpolating the velocities in the other plane. Then, the velocity gradient tensor is evaluated to obtain the vortex core by the λ_2–definition. The relationship between streamwise, longitudinal and spanwise vortices is systematically analyzed by overlapping the vortex lines and vortex cores and the whole flow topology is compared in both cases with and without an air spoiler. As a result, an air spoiler was found to weaken the C-pillar vortices producing strong wing tip vortices, which reduce downwash flow and longitudinal vortices increase in the vertical direction. The recirculation zone formed when an air spoiler is installed is higher and narrower than without a spoiler.

Keywords : particle image velocimetry (PIV), road vehicle, air spoiler, three-dimensional wake, vortex line, λ_2 method.

1. Introduction

Numerous numerical and experimental studies have been carried out to investigate the flow structures around a road vehicle. Although computational fluid dynamics using large eddy simulation (LES) method (Krajnovic and Davidson, 2004; Han, 1989) provided useful information on the aerodynamic characteristics such as the flow structure and the drag coefficient in the three-dimensional wake, but they still provide not that good results comparing with experimental ones for cases with complicated geometry and a high Reynolds number. To overcome this problem, a high performance parallel computing system is necessary as Tsubokura et al. (2006) used it to simulate flows around a formula car. Experiments by hot wire anemometry, laser Doppler anemometry, Pitot tube and multi-component balance (Ahmed et al., 1984; Kee et al., 2001) still have limitations on the analysis of the three-dimensional vortical structures despite showing reasonable data.

As the particle image velocimetry (PIV) technique that quantitatively visualizes the vortex structures (Zheng, 2007; Shao et al., 2007) has improved, many studies to examine the flow behavior around a road vehicle. Cogotti and Gregorio (2000) measured flow structures in the wake of a rearview mirror and around a frontal wheel of a full-size car. McCutchen et al. (2002) examined the wake characteristics of a simplified car model according to several angles of the hatchback. Al-Garni et al. (2003) and Heineck and Walker (1999) analyzed the turbulent flow around a truck by PIV measurements. However, these studies did not completely verify the whole wake phenomena including recirculation, but simply investigated the flow features. Recently, we reported on the PIV measurements in the wake of a downscaled sports car model at several sections and discussed the structural changes of the three-dimensional vortices caused by an air spoiler (Kim, et al., 2006), but we did not show the full three-dimensional vortical structure because of the lack of information on the out-of-plane velocity component.

Meanwhile, many strategies were tried to find out three-dimensional vortical structures for simple geometric flows. Perry and Chong (1987 and 1990) made a systematic approach that showed various vortical structures in two- or three-dimensional space using the critical point theory. Also, Jeong and Hussain (1995) suggested a vortical structure analysis method by the λ_2–definition, which has been regarded as the most practical tool to reveal the coherent structures of vortices under the incompressible flow condition.

The objective of the present study is to characterize the whole three-dimensional wake behind a road vehicle with the help of the λ_2 method and vortex line analysis, and to prove how an air spoiler changes the wake structures. Much of the sectional data were acquired using a PIV technique along the streamwise, spanwise and longitudinal axes and then the time-averaged data are calculated. These data on each plane are reconstructed three-dimensionally, including all the velocity components. The velocity component normal to the spanwise plane is obtained by interpolating the velocities in the longitudinal plane. The velocity gradient tensor is evaluated in all directions to get the three-dimensional vorticity components and the value of λ_2. After validating the identification method for vortex core by λ_2, sectional distributions are considered by overlapping with the streamlines and vortex lines. Finally, the structures and characteristics of vortices are discussed and the effects of an air spoiler on the flow fields are observed.

2. Experimental Setup and Scopes

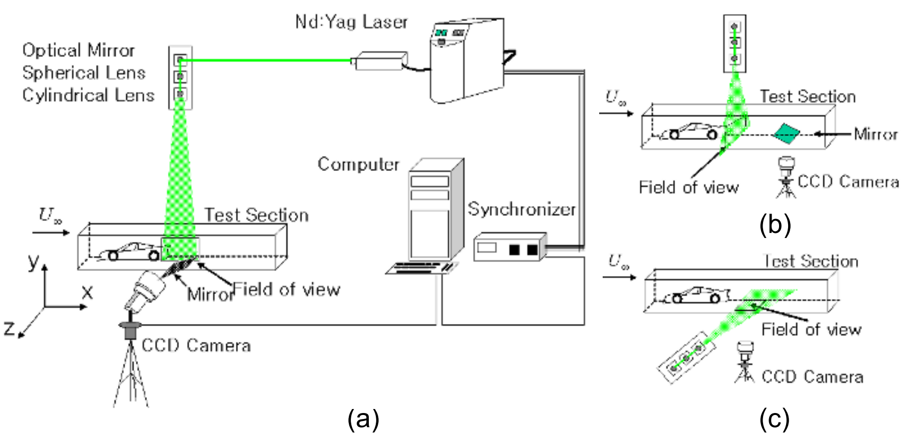

Fig. 1. Schematic diagram for (a) *x-y*, (b) *y-z* and (c) *z-x* plane measurements.

The present PIV system consists of a closed loop water tunnel, a dual head Nd-Yag laser (120 mJ), a CCD camera (1280 × 1024 pixels), a synchronizer and a computer for image processing as shown in Fig. 1. The experimental devices were set up as shown in Figs 1(a), (b) and (c) in order to obtain *x-y*, *y-z* and *z-x* plane data, respectively. The dimensions of the test section, which is made from transparent acryl, are 700 × 100 × 150 mm^3 (length × height × width). The thickness of the laser light sheet is 1 mm or 0.9 % of the characteristic length. Two otherwise identical vehicle models, with the only difference being the presence of an air spoiler, are fixed on the bottom surface of the test section. The CLK-GTR model vehicle (Mercedes Benz Inc.) scaled in the ratio of 1/43 is painted in lusterless black and has the dimensions of 112.86 × 25.56 × 45.35 mm^3. The Reynolds number based on the vehicle length is 10^5. Mean diameter of the seeding particle called hollow glass spheres is 10 μm. The air spoiler with the shape of an overturned airfoil is attached on the edge of the vehicle's trunk as depicted in Fig. 2. Boundary layer thickness in front of the vehicle is about 10 % of the vehicle height.

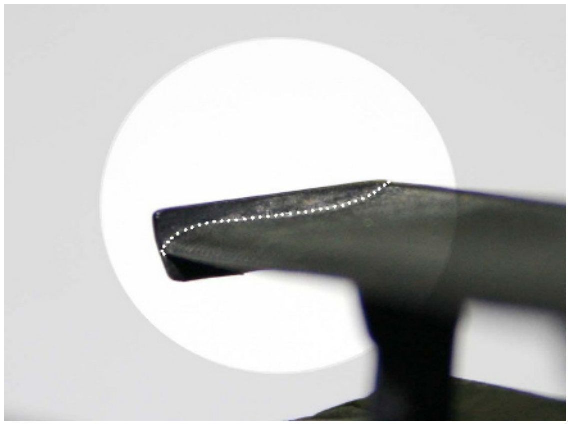

Fig. 2. Configuration of the air spoiler.

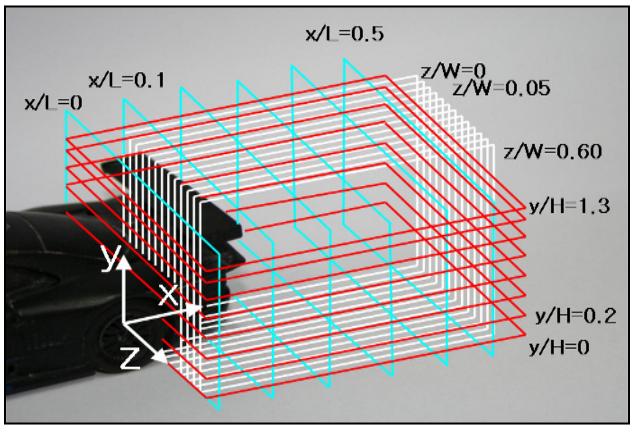

Fig. 3. Measurement planes behind a road vehicle.

Each of the x, y and z axes in Fig. 3 represents the direction of length (L), height (H) and width (W) of the vehicle, respectively. The origin is set at the leading edge of the air spoiler on the symmetric bottom plane. For the investigation of the spanwise vortices, thirteen x-y planes (63 × 50 mm^2) were measured from $z/W = 0$ (symmetric plane) to $z/W = 0.6$ at an interval of $z/W = 0.05$. Six y-z planes (46 × 70 mm^2), which were varied from $x/L = 0$ to $x/L = 0.5$ at an interval of $x/L = 0.1$, were measured to examine the streamwise vortices. Also, to study the longitudinal flow fields on the z-x plane, measurement were executed at the fourteen planes located from $y/H = 0$ (the bottom surface) to $y/H = 1.3$ at an interval of $y/H = 0.1$. A total of 488 instantaneous flow fields were captured at each plane and processed to obtain the time-averaged data. The magnification factors for the x-y, y-z and z-x plane were 20.0, 18.3 and 23.6 pixel/mm, respectively.

For the vector processing, a cross-correlation algorithm (Sung and Yoo, 2001) based on the fast Fourier transform (FFT) was applied and the interrogation windows with 32 × 32 pixels overlapped as much as 50 %. Also, window shifting and recursive correlation methods were adopted to enhance the signal-to-noise ratio. Finally, the velocity vector retained the spatial resolution of 1.3, 1.1 and 1.1 vector/mm for the x-y, y-z and z-x planes, respectively. See our previous work (Kim et al., 2006) for more details about the experimental system.

3. Results and Discussion

3.1 Three-Dimensional Wake and Vortex Identification

There have been many techniques to examine the three-dimensional vortical structures. The most general method is to take out the isovorticity surface from the absolute value of vorticity $|\omega|$. However, as this technique does not clearly show vortex cores in strong shear flows, the present study adopts the λ_2–definition proposed by Jeong and Hussain (1995), whose method is based on the fact that the minimum local pressure occurs at the vortex core. Here, the vortex core is defined as the region with the second largest negative eigenvalue of $S_{ij}^2+\Omega_{ij}^2$, where $S_{ij}=\frac{1}{2}(u_{i,j}+u_{j,i})$ is the strain-rate tensor and $\Omega_{ij}=\frac{1}{2}(u_{i,j}-u_{j,i})$ is the rotation-rate tensor. To obtain the vortical structure through the λ_2–definition, all the three-dimensional velocity components are needed and these are computed by combining the sectional data. The velocities u and v are used from the x-y plane data and the velocity w is extracted from the z-x plane data by the Lagrange interpolation method based upon a linear shape function for a brick element. Finally, the velocity gradient tensor $u_{i,j}$ and the vorticity components (ω_X, ω_Y, ω_Z) are calculated from the three-dimensional velocity field data to obtain the second largest eigenvalue λ_2 and the absolute value of vorticity.

(a) Without an air spoiler (b) With an air spoiler

Fig. 4. Streamline patterns of the three-dimensional velocity field.

In Fig. 4, Three-dimensional streamline patterns are plotted using the reconstructed velocity fields of the wake behind a road vehicle. The size of the recirculation zone without the air spoiler (Fig. 4(a)) is relatively small compared with that with the air spoiler (Fig. 4(b)). Shear flows from the trunk and lateral sides of the vehicle wrap the recirculation zone. Meanwhile, when an air spoiler is equipped on the trunk, the wing tip vortices generated at both edges of the air spoiler have a dominant effect on the wake in the ways they lift the surrounding fluid.

(a) Without an air spoiler (b) With an air spoiler

Fig. 5. Isosurfaces of the absolute vorticity |ω| reconstructed from the x–y and z–x plane data.

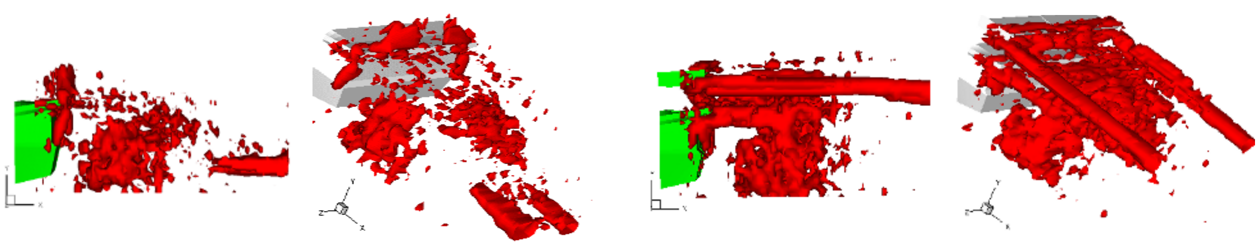

(a) Without an air spoiler (b) With an air spoiler

Fig. 6. Isosurfaces of λ_2 in different views calculated from the three-dimensionally reconstructed data.

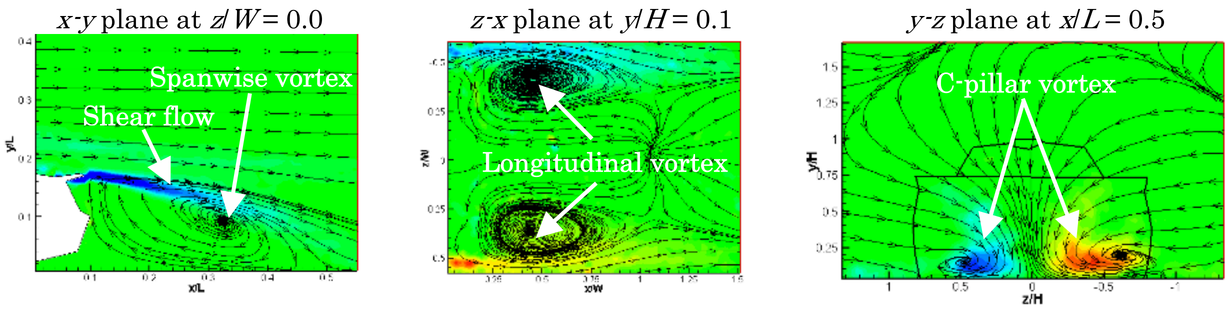

(a) Without an air spoiler

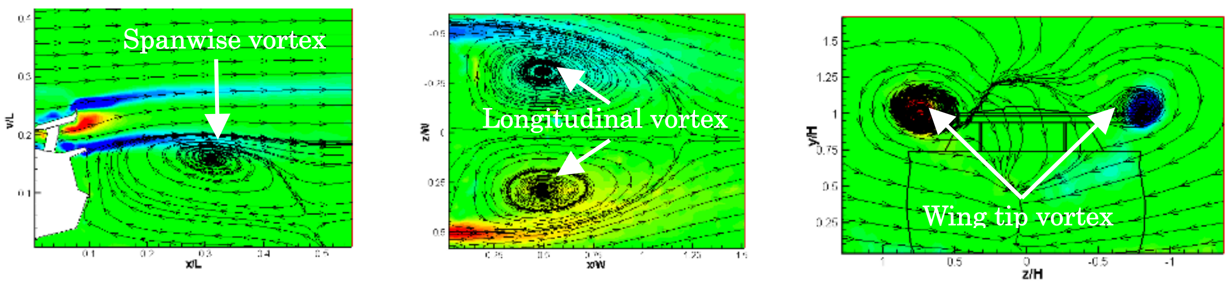

(b) With an air spoiler

Fig. 7. Streamlines overlapped with vorticity contour in each plane (a) without an air spoiler and (b) with an air spoiler.

Isosurfaces of $|\omega|$ and λ_2 plotted at different views in Figs 5 and 6. The $|\omega|$–definition has merit in that it shows simultaneously all of the vortical motions, but its isosurface is governed by the largest among the three-dimensional vorticity components. Thus, in Fig. 5, the vortical structure within the recirculation zone is not seen because of large values of the velocity gradient and vorticity by shear flows. In other words, the isosurfaces of $|\omega|$ only show some parts of streamwise vortices formed along the shear flows, and do not show the spanwise and longitudinal vortices inside the recirculation region. On the other hand, the λ_2–definition can show precisely complicated vortical structures in the recirculation zone without expressing shear flow. Figure 6 depicts the distribution of λ_2 in two eye views to identify the effect of an air spoiler on the wake.

To verify the vortex identification by the λ_2-definition, the contours of vorticity and λ_2 overlap the sectional streamlines in Fig. 7 and 8. The vorticity contours in Fig. 7 result from two-dimensional data obtained in our previous work (Kim et al., 2006) and λ_2 contours in Fig. 8 show the sectional views of the three-dimensional data. It is clearly seen from the streamlines that there exists three types of vortex; a spanwise vortex in the *x-y* plane, a pair of longitudinal vortices in the *z-x* plane, and a pair of C-pillar or wing-tip vortices in the *y-z* plane. In the *x-y* plane of Fig. 8, the core of a large spanwise vortex is exactly coincident with the center of the λ_2 contours. However, in Fig. 7, the region of large vorticity appears in the shear flow as separated at the vehicle trunk, because the velocity gradient is high in this region, not inside the spanwise vortex. Regarding the *z-x* and *y-z* planes of Fig. 8, the centers of longitudinal and streamwise vortices are also located at the centers of the λ_2 contours. Therefore, the evaluation of the three-dimensional vortex structures given in Fig. 6 is reasonable. The C-pillar vortices shown in the *y-z* plane for the case without an air spoiler, separate at the top side of the rear window and travel downstream in the wake of a notchback vehicle (Gilhome et al., 2001). On the other hand, with an air spoiler, they are remarkably weakened and nearly disappear because of strong streamwise wing tip vortices with opposite rotational direction, as shown in the figure of Fig. 8(b) (Kim et al., 2006).

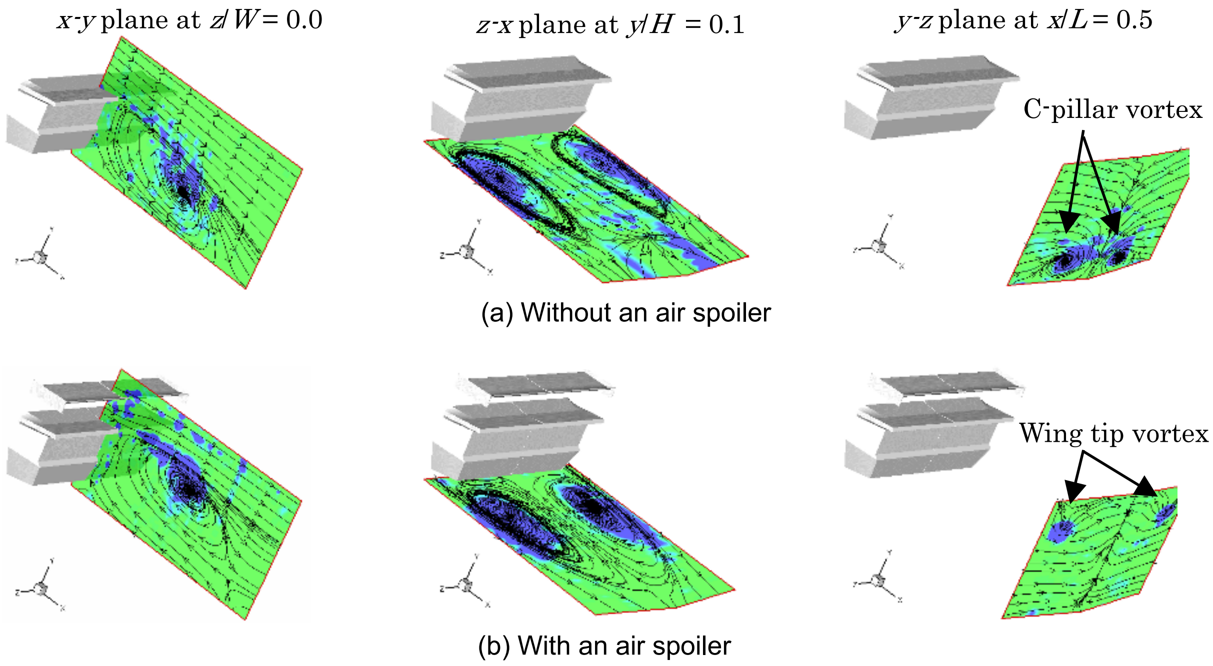

Fig. 8. Streamlines overlapped with λ_2 contours (a) without an air spoiler and (b) with an air spoiler.

3.2 Characteristics of Vortices

Since the wake of a road vehicle is intrinsically three-dimensional accompanied with complex vortices, a systematic analysis on the flow kinematics is required to characterize the flow. Visualizing the flow by streamlines is undoubtedly one of the clever methods, but it is hard to make out the structures only by the streamlines when the flows are three-dimensional. In the present study, a concept of the vortex line, which is a line whose tangents are parallel everywhere to the vorticity vector, is applied in conjunction with the streamline. Since the vorticity vector is divergence-free, the vortex line is considered as a kind of material line and circulation is conserved along the vortex tube. The vortex line analysis has the merit that it does not depend on the frame of reference, because vorticity is obtained from the derivative of velocity.

In Fig. 9, streamlines and vortex lines are plotted with the contours of λ_2 for each plane. For each set of the streamlines and vortex lines, the figures on the left are the results without an air spoiler and the figures on the right are the results with an air spoiler. First of all, in the x-y plane of $z/W = 0.4$ (Fig. 9(a)), the λ_2 distributions show that a large longitudinal vortex is formed just behind the rear side. This vortex results from the separated shear flow at the sidewall. With an air spoiler, it is clearly seen that a wing tip vortex is stretched to the downstream. Even though the streamlines in Fig. 9(a) do not describe the longitudinal and wing tip vortices, the vortex lines clearly show the direction of vortices. The direction of the arrow is the axis of rotation. In the region of longitudinal vortex, the vortex lines go upward (the y direction) and in the region of the wing tip vortex, they face downstream (the x direction). Note that without an air spoiler the vortex lines go upstream because of the existence of C-pillar vortices. Figure 9(b) shows the results of the z-x plane of $y/H = 0.7$. The wing tip and spanwise vortices occur with the air spoiler. The vortex lines in this figure are in the negative z direction because of the spanwise vortex and in the positive x direction because of the wing tip vortex. Without the air spoiler, the spanwise vortex is observed at $y/H = 0.5$-0.6 but it disappears at $y/H = 0.7$ and instead the shear flow separated on the trunk is dominant. Thus, the vortex lines are straightforward because of the strong shear flow. Figure 9(c) shows the results of the y-z plane of $x/L = 0.2$. Without an air spoiler, large longitudinal and small C-pillar vortex pairs are found. On the other hand, an additional strong wing tip vortex pairs exists when the air spoiler is present. It is interesting to see that without an air spoiler, the streamlines in Fig. 9(c) converge to a nearby center of the plane. However, in the presence of an air spoiler, they go upward along the symmetry line

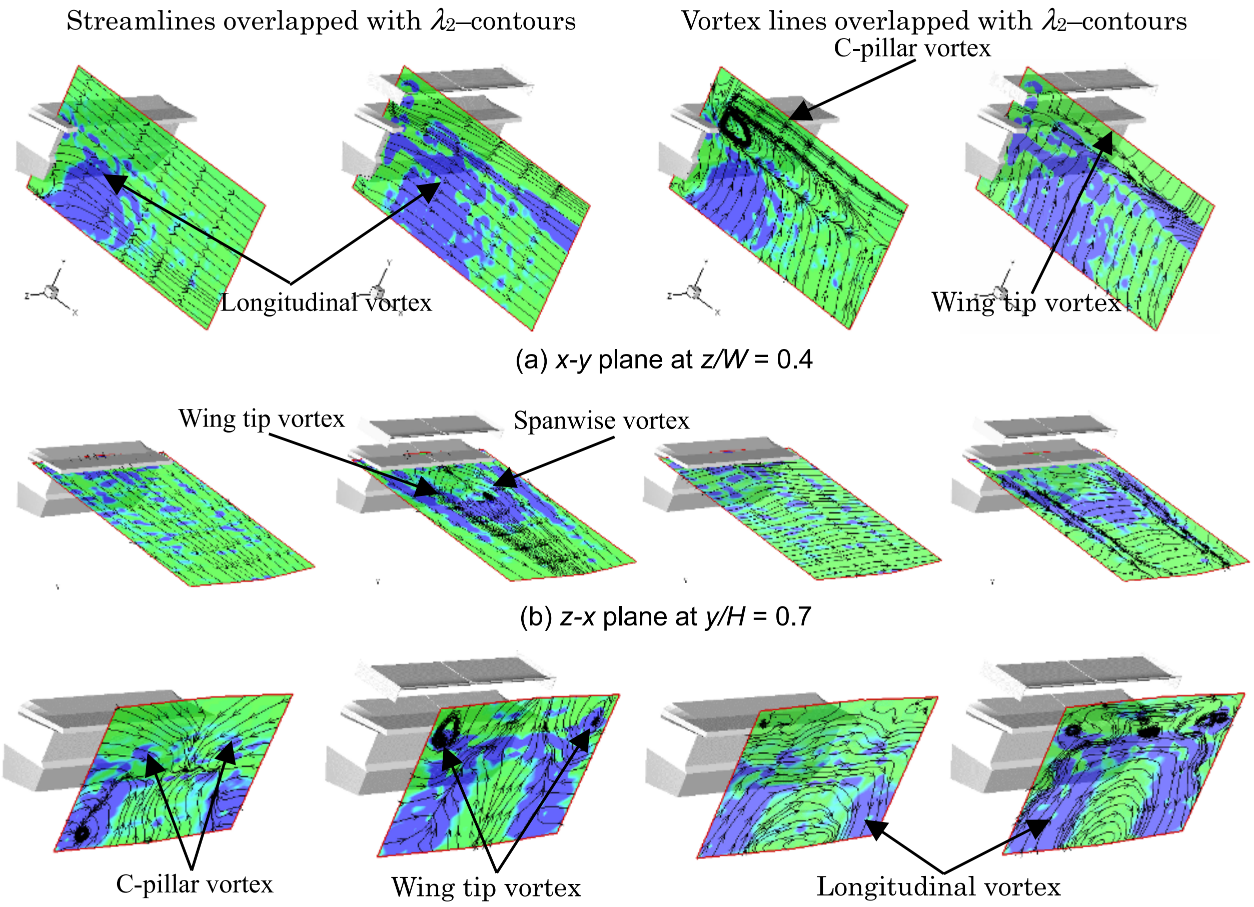

Fig. 9. Streamlines and vortex lines overlapped with λ_2–contours in the (a) x-y, (b) z-x and (c) y-z planes. For each set of the streamlines and vortex lines, the figures on the left are the results without an air spoiler and the figures on the right are the results with an air spoiler.

because of the wing tip vortices. Meanwhile, the vortex lines circulate around the bottom center of the plane. The upward and downward vortex lines on the left and right sides are a result of the longitudinal vortices. The horizontal vortex lines in the upper side are because of shear flow. As a result, no vortex appears in the central bottom region, since the spanwise vortex does not govern the flow at $x/L = 0.2$. The existence of the wing tip vortices causes the circulating vortex line to soar.

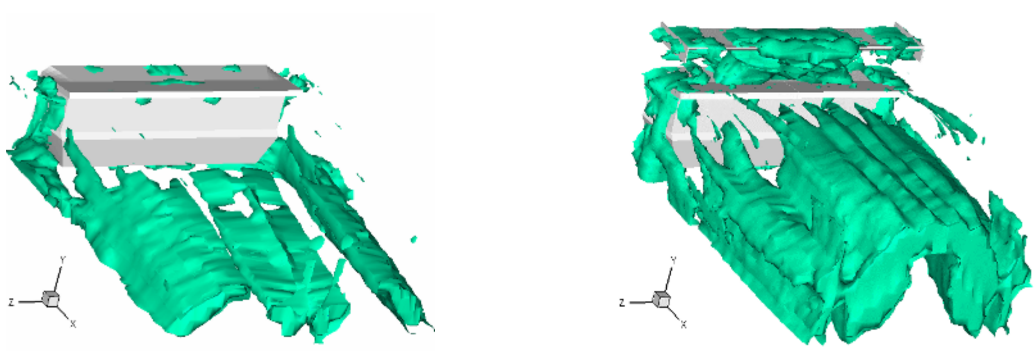

(a) Without an air spoiler (b) With an air spoiler

Fig. 10. Isosurfaces of turbulence kinetic energy (a) without and (b) with an air spoiler.

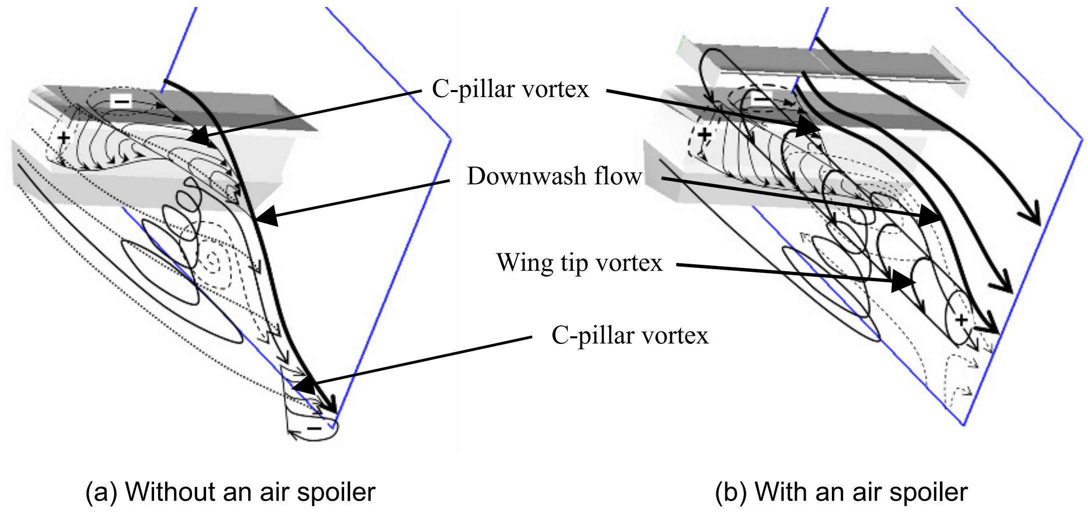

Fig. 11. Flow topology in the wake behind a vehicle (a) without and (b) with an air spoiler.

Since the wake is unsteady turbulent flow, turbulence kinetic energy $k=\frac{1}{2}(u'^2+v'^2+w'^2)$ is plotted in Fig. 10 and compared for the cases with and without an air spoiler. The value of isosurface is set to be 0.048 m^2/s^2. From this figure, it is evident that the air spoiler produces much more turbulence kinetic energy. A point in common for both the cases is that turbulence kinetic energy is highly concentrated in the region of the longitudinal vortex, which is the strongest one in the wake. The shapes of isosurfaces closely resemble the vortex lines observed in the y-z plane. However, in the central region, the high turbulence energy is distributed oppositely for both the cases. Without an air spoiler, it happens at the bottom, but with an air spoiler, it goes upward. The main reason is that the role of C-pillar and wing-tip vortices is different. The former pushes down the wake by entraining upside fluid and the latter attracts it to the upper direction.

From the above analysis of the vortex lines and vortex cores, the topological flow structures on the wake behind the road vehicle are depicted in Fig. 11. C-pillar vortices are found on the trunk for both cases but they show different behavior on the wake. For the case without an air spoiler (Fig. 11(a)), the C-pillar vortices induce strong downwash flow that suppresses the growth of the longitudinal vortices. Thus, the flows separated from the lateral side circulate within the recirculation zone and merged into the C-pillar vortices at the downstream. However, when the air spoiler is installed, as drawn in Fig. 11(b), strong wing tip vortices generated from both edges of the air spoiler are dominant and weaken the C-pillar vortices. In addition, this causes the longitudinal vortices to be stronger which are separated from the lateral sides with reducing the downwash flow. As a result, with the air spoiler the recirculation zone is formed higher in the vertical direction and narrower in the spanwise direction.

In the present study, drag and lift forces are not measured but Kee et al. (2001) mentioned that lift was decreased by reducing the magnitude of C-pillar vortices when an air spoiler or a trunk lid kick-up was installed. They also found that an air spoiler or kick-up might reduce drag force if it was properly designed. Cogotti and De Gregorio (2000) reported that the stronger the C-pillar vortices were formed, the more downwash flow was generated. In this experiment, the same phenomenon is observed as explained above. Thus, by an air spoiler, the present vehicle model could have a negative lift force, which contributes to the driving stability.

4. Conclusions

The time-averaged velocity fields formed in the wake of a road vehicle have been measured on the several planes along each axis using a PIV technique. To describe the vortical structures completely, full three-dimensional velocity fields were reconstructed. The present study proved that the vortical structures could not be identified by the isosurface of absolute vorticity, since the shear flow is strong in the wake of a road vehicle. Instead, by means of the λ_2–definition, they could be captured inside the recirculation zone as well. Furthermore, the vortex lines can indicate the direction of rotation. By overlapping with the vortex core defined by λ_2, complex vortices, which are linked to each other, are successfully discriminated in both cases, with and without an air spoiler. The resultant change of flow topology by the existence of an air spoiler is as follows; without an air spoiler, spanwise, longitudinal and C-pillar vortices are observed separately, but the result with an air spoiler shows that C-pillar vortices are weakened and strong wing tip vortices are formed instead. The main role of the wing tip vortices is to reduce the downwash flow, which causes the longitudinal vortices generated from the lateral sides to be higher.

Acknowledgement

This work was supported by the NURI project of the Ministry of Education, Korea in 2007. The authors would like to thank the Seoul Metropolitan Government for their support and interest in this work through Strategic Industry Innovation Cluster Program.

References

Ahmed, S. R., Ramm, G. and Faltin, G., Some Salient Features of the Time-Averaged Ground Vehicle Wake, SAE Paper, 840300 (1984).
Al-Garni, A. M. and Bernal, L. P., Experimental Investigation of the Near Wake of a Pick-up Truck, SAE Paper, 2003-01-0651, (2003).
Chong, M. S. and Perry, A. E., A General Classification of Three-Dimensional Flow Fields, Phys. Fluids A, 2-5 (1990), 765-777.
Cogotti, A. and De Gregorio, F., Presentation of Flow Field Investigation by PIV on a Full-Scale Car in the Pininfarina Wind Tunnel, SAE Paper, 2000-01-0870, (2000).
Han, T., Computational Analysis of Three-Dimensional Turbulent Flow around a Bluff Body in Ground Proximity, AIAA Journal, 27-9 (1989), 1213-1219.
Gilhome, B. R., Saunders, J. W. and Sheridan, J., Time Averaged and Unsteady Near-Wake Analysis of Cars, SAE Paper, 2001-01-1040, (2001).
Heineck, J. T. and Walker, S. M., 3D PIV in Wind Tunnel Applications: Measurements of a Truck Wake, SAE Paper, 1999-01-5600, (1999).
Jeong, J. and Hussain, F., On the Identification of a Vortex, Journal of Fluid Mechanics, 285 (1995), 69-94.
Krajnovic, S. and Davidson, L., Large-Eddy Simulation of the Flow around Simplified Car Model, SAE Paper, 2004-01-0227, (2004).
Kee, J. D., Kim, M. S. and Lee, B. C., The Coanda Flow Control and Newtonian Concept Approach to Achieve Drag Reduction of Passenger Vehicle, SAE Paper, 2001-01-1267, (2001).
McCutcheon, G., McColgan, A. H., Grant, I. and Hurst, D., Wake Studies of a Model Passenger Car Using PIV, SAE Paper, 2002-01-3335, (2002).
Kim, J. S., Kim, S., Sung, J., Kim, J. S., and Choi, J., Effects of an Air Spoiler on the Wake of a Road Vehicle by PIV Measurements, Journal of Visualization, 9-4 (2006), 411-418.
Perry, A. E. and Chong, M. S., A Description of Eddying Motions and Flow Patterns Using Critical-Point Concepts, Ann. Rev. Fluid Mech., 19 (1987), 125-155.
Shao, C. P., Wang, J. M. and Wei, Q. D., Visualization Study on Suppression of Vortex Shedding from a Cylinder, Journal of Visualization, 10-1 (2007), 57-64.
Sung, J. and Yoo, J. Y., Three-Dimensional Phase Averaging of Time-Resolved PIV Measurement Data, Meas. Sci. Technol., 12 (2001), 655-662.
Tsubokura, M., Kobayashi, T. and Oshima, N., High Performance Computation of Unsteady Flow Around a Formula Car Using Large-scale LES on Earth Simulator, 12th International Symposium on Flow Visualization, (2006-9).
Zheng, Y., The Visualization of Three-Dimensional Vortex Structures in a Mixing Layer, Journal of Visualization, 10-1 (2007), 33-36.

Author Profile

Jin Seok Kim: He obtained his master degree of engineering in mechanical engineering from Sunchon National University, Korea in 2005 and is currently a Ph.D. candidate in the same university.

Jaeyong Sung: He received his master and Ph.D. degrees in mechanical engineering in 1996 and 2001, respectively from Seoul National University, Korea, and worked for Digital Appliance Laboratory of LG Electronics Inc. as a senior researcher. Also he taught in mechanical and automotive engineering of Sunchon National University as a professor. And he has been working in department of mechanical engineering in Seoul National University of Technology as a professor since 2004. His research interests are all the areas related to PIV technology, hemodynamics, biochips, rarefied gas flow with DSMC, etc.

Sungcho Kim: He received his master and Ph.D. degrees in aeronautical engineering in 1985 and 1989, respectively from KAIST, Korea, and worked in Central Technology Institute of Daewoo Heavy Industry Ltd. He researched in Mississippi State University and University of California, Santa Barbara as a visiting scholar in 1994 and 2000, respectively. And he served as the dean in college of engineering, Sunchon National University, and has been working in school of mechanical and aerospace engineering in Sunchon National University as a professor since 1989. His research area is experimental and computational fluid engineering.

Jeong Soo Kim: He received his master and Ph.D. degrees in aeronautical engineering in 1987 and 1992, respectively from KAIST, Korea, and worked for KIMM, ADD, and KARI as a principal researcher. Also he researched in TRW(USA) as an assistant program manager from 1996 to 1998. And he has been a faculty member in school of mechanical and aerospace engineering in Sunchon National University since 2004. His research interests are satellite propulsion system, measurement and visualization of injector spray pattern using PDA, combustion, test and evaluation of liquid rocket engine, etc.